Available online at www.sciencedirect.com
SCIENCE DIRECT®

Journal of the European Ceramic Society 24 (2004) 189–195

www.elsevier.com/locate/jeurceramsoc

Low-cost preparation of Si_3N_4–SiC micro/nano composites by in-situ carbothermal reduction of silica in silicon nitride matrix

Miroslav Hnatko*, Dušan Galusek, Pavol Šajgalík

Institute of Inorganic Chemistry, Slovak Academy of Sciences, Dúbravská cesta 9, SK-845 36 Bratislava 45, Slovak Republic

Abstract

SiC/Si_3N_4 nano/micro composites were prepared from a mixture of α-Si_3N_4, amorphous carbon (carbon black), and Y_2O_3 by carbothermal reduction of SiO_2 present at the surface of Si_3N_4 matrix grains, or added deliberately to the starting mixture. A special heating regime allowed the outgassing of CO(g) (a product of carbothermal reduction) and reduced the residual porosity to less than 2%. The inter- and intragranular SiC inclusions containing the amorphous oxygen-rich layer at the interface between SiC and the Si_3N_4 grains were present, originating from the reaction of free carbon with the silica melt. The reaction consumes silica in the grain boundary phase. The change of the grain boundary chemistry influences both room and high temperature properties of the nanocomposite.

Keywords: Inclusions; Mechanical properties; Nanocomposites; SiC; Si_3N_4

1. Introduction

Materials based on the nanocomposite concept described by Niihara,[1] show excellent bending strength,[2] which is accompanied by a modest increase of fracture toughness and improved creep behaviour.[3] However, fabrication of nanocomposite materials by a traditional processing route of mixing the submicrometre Si_3N_4 and SiC powders followed by hot pressing or pressureless sintering is sometimes problematic and often does not yield expected results. Other ways of fabrication of the nanocomposites have therefore been reported. In our previous work[4] the SiC nanoinclusions were formed by in situ decomposition and crystallisation of a polymer-derived amorphous SiNC powder. Although the amorphous SiNC powder reportedly contained significant amount of free carbon,[5] very little carbon could be detected within the microstructure of the composite, which consisted of elongated micrometer-sized grains of Si_3N_4, intergranular submicrometre grains of SiC and two types of nano-sized SiC inclusion within the Si_3N_4 grains. The intragranular SiC inclusions were either directly embedded within the Si_3N_4 matrix with clean SiC/Si_3N_4 interface, or surrounded by an oxygen-rich amorphous layer, which suggested their origin was different. No free carbon could be detected within the matrix. One order of magnitude higher creep resistance was measured for the composite than for the reference material with identical amount and composition of sintering additives, but without SiC. The change of the creep mechanism from the grain boundary glass weakening to diffusion-controlled creep was also observed. It is concluded, that the free carbon introduced as an intrinsic component of the amorphous SiCN influences the microstructure and properties of the composite in two ways: (1) free carbon reacts with SiO_2, which is always present at the surface of the Si_3N_4 grains at the formation of SiC. The SiC inclusions surrounded by the amorphous oxygen and yttrium-rich layer result from the process. (2) Depleting the grain boundary glass of silica both reduces the amount of grain boundary glass and shifts the composition of glass to the region with higher eutectic temperature according to the SiO_2–Y_2O_3 phase diagram.[6]

In order to elucidate the function of free carbon in the glass-forming binary system SiO_2–Y_2O_3 used as the sintering aid, a set of model experiments has been carried out.[7] The molar ratio of $SiO_2/Y_2O_3 = 2.57$ corresponding to the lowest eutectic temperature 1660 °C of the system has been used. The XRD measurements confirmed the presence of SiC in the SiO_2–Y_2O_3–C system

* Corresponding author.
E-mail address: uachmiho@savba.sk (M. Hnatko).

0955-2219/$ - see front matter © 2003 Elsevier Ltd. All rights reserved.
doi:10.1016/S0955-2219(03)00604-6

after heat treatment, when the C/SiO_2 molar ratio was close to 3 or higher. The carbothermal reduction of silica at the increased carbon content in the starting mixture and formation of SiC increased the melting temperature of the system from 1660 to 1900 °C, due to the shift of the composition from the region of the SiO_2–$Y_2Si_2O_7$ eutectic to the region of the eutectic of the pseudobinary system $Y_2Si_2O_7$–$Y_4Si_3O_{12}$ (1900 °C).

These results indicate, that addition of free carbon provides an opportunity of preparation of silicon nitride–silicon carbide micro/nano composite with increased creep resistance by the in situ reaction of carbon with silica under the conditions routinely applied in the process of densification. Carbon added in the form of soot or as an organic precursor (e.g. sacharose), which yields carbon as a result of pyrolytic cracking of the carbon chain without the presence of oxygen are much cheaper than the amorphous polysilazane-derived SiCN powder. This provides a way of low-cost preparation of the composite.

This work deals with low-cost preparation of the Si_3N_4–SiC micro/nano composite by the *in situ* carbothermal reduction of silica within the silicon nitride matrix. The room and high temperature mechanical properties of the material are also discussed.

2. Experimental

Two different compositions were studied in the present work. The compositions are listed in Table 1. In both the SNYC1 and SNYC2 samples the molar ratio of SiO_2 to Y_2O_3 was set to 2.57, corresponding to the lowest eutectic temperature in the SiO_2–Y_2O_3 system (1660 °C). Free carbon was added in the amount sufficient for elimination of silica within the material. The sample SNYC2 contained an extra 5.96 wt.% of SiO_2 and 3.62 wt.% C in order to create 5wt.% SiC by carbothermal reduction of silica.

The powders were mixed and homogenised in a polyethylene bottle with Si_3N_4 spheres in isopropanol for 24 h. Homogenised slurries were dried and sieved through 25 μm sieve in order to eliminate large hard agglomerates. The powders were uniaxially pressed in a steel die at 30 MPa and green discs with the diameter of 48 and 5 mm thick were prepared. The discs were embedded in a BN powder bed and placed in a graphite die. The samples were then hot-pressed using a specific schedule, which included variation of heating rates, gas pressure in the furnace and applied mechanical pressure. The schedule was designed in order to allow for completion of the carbothermal reduction of silica and for proper outgassing of the reaction products (CO) before densification is complete. The heating schedule is shown in Fig. 1. The background for the use of specific conditions in the course of preparation of the specimens is discussed below (see Results and discussion). Hot-pressed discs were cut and the faces of rectangular bars with dimension 3×4×45 mm were polished with a diamond paste to 1 μm finish. Density was measured by the mercury immersion method. Polished samples were etched in the Polaron plasma barrel etcher PT 7150. The etched surfaces were examined by SEM (Jeol JSM-35), and the elemental analysis was conducted using energy disperse spectrometry (EDX, Cambridge, UK). The crystalline phases were identified by X-ray diffraction (XRD) (powder diffractometer STOE with CoK_α radiation). The microstructure and the sub-grain inclusions were investigated by transmission electron microscopy (TEM). Analytical transmission electron microscopy (EFTEM) was performed using a GATAN imaging filter mounted on a Philips CM20/STEM (acceleration voltage 200 keV; equipped with a LaB_6 cathode).

The hardness was measured on polished cross-sections of the bars using the standard Vickers indentation technique at the load of 10 N. The fracture toughness was estimated from the length of cracks introduced by Vickers indentation at the load of 100 N by the method described by Shetty.[8]

Table 1
Composition of starting powders (wt.%)

Sample	Si_3N_4[a]	Y_2O_3[b]	C[c]	SiO_2[d]	SiCN[e]
SNYC1	93.23	4.91	0.43	1.43	–
SNYC2	84.12	4.43	0.43 + 3.62	1.43 + 5.96	–
SNY	95.00	5.00	–	–	–
SNY20	75.00	5.00	–	–	20

[a] UBE E10, Tokyo, Japan: oxygen content 1.1 wt.%, carbon content 0.15 wt.%.
[b] PIDC 99.99%, An Arbor, MI, USA.
[c] Carbon black, pigment grade, 1000 $m^2\ g^{-1}$.
[d] Aerosil OX-50, Degusa, Germany: 50 $m^2\ g^{-1}$.
[e] Prepared at the TU Darmstadt, Germany.

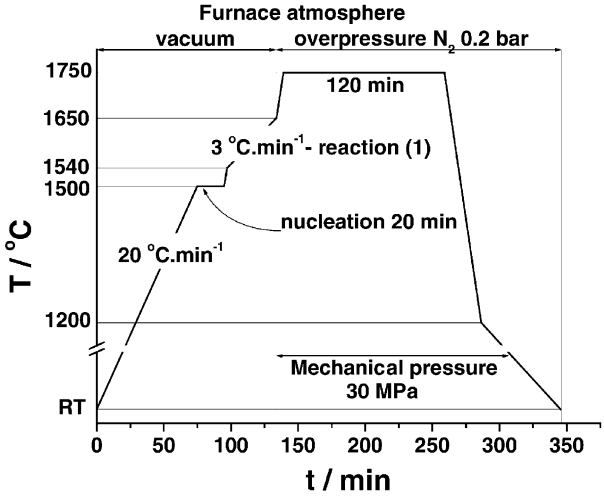

Fig. 1. The schematic of thermal treatment during the *in situ* formation of SiC followed by densification of the material.

The room temperature bending strength was measured on the (45×5×3) mm^3 rectangular bars with tensile face polished to 15 μm finish at the crosshead speed of 0.5 mm/min and inner/outer span 20/40 mm, respectively.

The creep tests in flexure (20/40 inner/outer span) were carried out in air in the temperature range between 1200 and 1400 °C, with a step of 50 °C. The stepwise load increase was applied at each temperature. The creep experiment started with a load of 50 MPa. After 24 h dwell time the load was increased to 100 MPa for the next 24 h and then to 150 MPa for the last 24 h in order to speed up the collection of data. The only exception was the sample SNYC2 where the 50 h dwell times were used at each applied load.

The specimens SNY and SNY20 from our previous work[4] were used as the references. For details on composition, see Table 1.

3. Results and discussion

Reduction of SiO_2 in the SiO_2–Y_2O_3 system is possible when activity of carbon is high ($a_C \leqslant 1$):[9,10]

$$\begin{array}{l} SiO_2(s,l) + 3C(s) \rightarrow SiC(s) + 2CO(g) \\ K_1(1540\ ^\circ C) = 2.3 \qquad \Delta G_1(1540^\circ C) = -12.3\ \text{kJ/mol} \\ K_1(1750^\circ C) = 97.3 \qquad \Delta G_1(1750^\circ C) = -77.0\ \text{kJ/mol} \end{array} \quad (1)$$

Formation of CO(g) by the reaction (1) within the bulk composite is problematic. Evolved gas can be entrapped in the closed pores and hinder densification, in the worst case causing formation of cracks, if the pressure within the pores exceeds locally the strength of the material.

Another source of SiC is the reaction of silicon nitride with carbon, which at normal pressure of nitrogen proceeds at temperatures exceeding 1440 °C:[11]

$$\begin{array}{l} \alpha\text{-}Si_3N_4(s) + 3C(s) \rightarrow 3\beta\text{-}SiC(s) + 2N_2(g) \\ K_2(1540^\circ C) = 2.2 \qquad \Delta G_2(1540^\circ C) = -32.5\ \text{kJ/mol} \\ K_2(1750^\circ C) = 5.4 \qquad \Delta G_2(1750^\circ C) = -91.6\ \text{kJ/mol} \end{array} \quad (2)$$

The hot-pressing regime shown in Fig. 1 was designed on the basis of preliminary thermodynamic calculations. Nucleation of SiC took place at 1500 °C in vacuum. According to the calculations performed the temperature was sufficiently high for both reactions (1) and (2) to start and proceed at sufficiently low rate and to facilitate the formation of the required number of nuclei. At this temperature the porosity of the silicon nitride matrix was still high and the small amounts of CO and N_2 formed during the nucleation of SiC were readily outgassed. The 20 min nucleation period was followed by rapid increase (20 °C/min) of the temperature to 1540 °C followed by slow heating to 1650 °C at 3 °C/min. During this period, the nuclei were allowed to grow. The slow heating rate was deliberately selected to provide sufficient time for removal of the gaseous reaction products CO and N_2. The end of the reactions (1) and (2) and of the CO and N_2 outgassing, i.e. the completion of the carbothermal reduction of silica was detected by monitoring the level of vacuum in the furnace. As soon as the vacuum was restored to its original value, it was assumed no more gases are formed and the reactions were completed. The mechanical load of 30 MPa was then applied at 1650 °C, and the temperature increased rapidly to 1750 °C, in order to facilitate fast densification of the silicon nitride matrix with highly refractory (yttria-rich) grain boundary phase and to prevent grain growth. The slight overpressure of N_2 (0.2 bar) was applied in order to hinder thermal decomposition of Si_3N_4:

$$Si_3N_4 \rightarrow 3Si + 2N_2 \quad (3)$$

The final densities of the SNYC1 and SNYC2 samples achieved 3.23 and 3.21 g cm^{-3}, which represent 99 and 98% respectively of the theoretical value calculated by the rule of mixtures.

3.1. Microstructure

The SEM micrographs of the SNYC1 and SNYC2 samples are shown in Fig. 2, together with the micrographs of the reference samples SNY and SNY20. In all cases the materials consist predominantly of elongated β-Si_3N_4 grains with equivalent circle diameter between 0.3 and 0.8 μm and with aspect ratio close to 3 surrounded by a continuous amorphous grain boundary phase. In the case of composite samples, nanometre sized inclusions β-SiC are observed inside the Si_3N_4 grains. The presence of crystalline β-SiC in the material was confirmed by XRD measurement. Except SiC, clusters of unreacted carbon could be seen throughout the microstructure of composite samples. Free carbon was present either in the form of individual particles approximately 0.2 μm in diameter, or in the form of clusters with diameter approximately 15 μm. This feature is especially pronounced in case of the SNYC1. The microstructures of both carbon-derived composites are finer than the microstructures of the monolithic Si_3N_4 (SNY) or the SiNC-derived nanocomposite (SNY20).

The results of TEM analysis of intragranular inclusions coupled with the EFTEM mapping is shown in Fig. 3. The interesting feature revealed by the EFTEM mapping is, that the inclusion is surrounded by an oxygen-rich layer containing practically no silicon. Taking into account the composition of oxide sintering additives in the system, it is suggested[12] that the layer consist predominantly of yttria, as the residue of the yttria–silica melt. Silica originally present in the melt was con-

sumed when the SiC inclusion was formed by carbothermal reduction. Direct experimental evidence has been reported recently, when the SiC nanoparticles in the intimate contact with residual amorphous carbon surrounded by an amorphous, yttria-rich phase has been detected in a Si_3N_4–SiC micro/nano composite.[13]

3.2. RT mechanical properties

The measured mechanical properties are listed in Table 2. The fracture toughness of all nanocomposites was lower than the fracture toughness of monolithic Si_3N_4 sample SNY. This can be most likely attributed to small number of *intra* SiC inclusions. As documented recently,[14] the *intra* inclusions of the second phase with different thermal expansion coefficient than that of the matrix phase can have a positive effect on the fracture toughness of two phase composite. The presence of such *intra* grains results in formation of significant residual stresses within the silicon nitride matrix, which were found to be compressive in nature.[4] Although the exact function of the residual stresses in nanocomposites as not established with certainty, their importance with respect to the mechanical properties is already widely accepted and is studied worldwide. It has been also shown, that there exist the optimum fraction of SiC, which results in excellent room temperature properties of the material. The optimum lies between 5 and

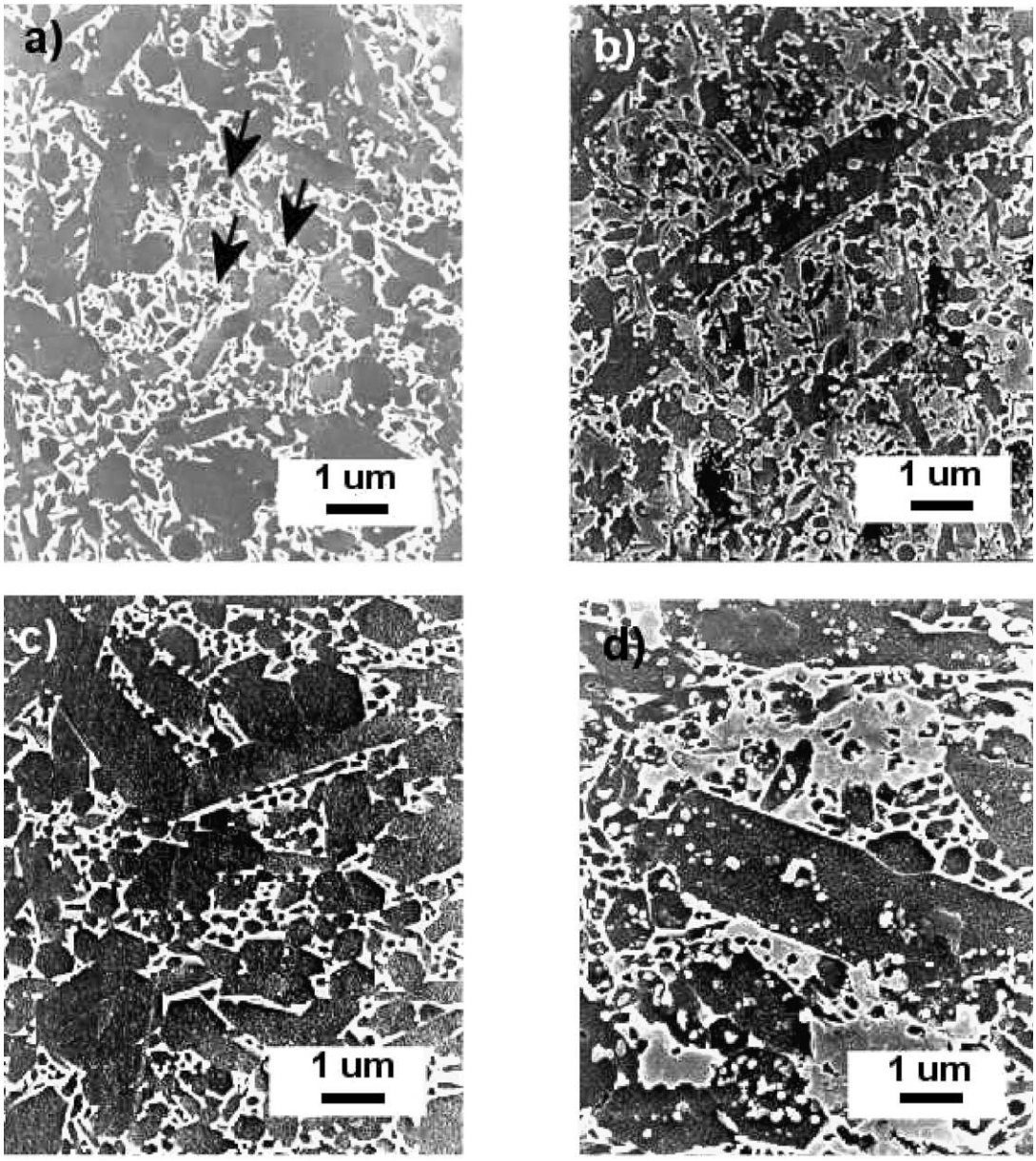

Fig. 2. The SEM micrographs of the the SNYC1 (a) and SNYC2 (b) samples and of the reference specimens SNY (c) and SNY20 (d). The inclusions of unreacted carbon are marked by the arrows.

10 wt.%.[15] The composites studied, however contain in theory a maximum of 5 wt.% of SiC grains in total, provided the carbothermal reduction of silica was complete. This is obviously not true, as free carbon clusters could be detected within the matrix (Fig. 4). Moreover, part of the inclusions is expected to remain *outside* the Si_3N_4 grains, similar to the SNY20 reference material.[4] The effective number of the *intra* SiC inclusions is then much lower than the optimum value mentioned above. It has also been documented, that the strain fringes in the Si_3N_4 grains arise from the presence of SiC nano-inclusion with "clean" interface, i.e. without the surface oxygen-rich layer.[4] These are formed by re-crystallisation of the amorphous SiNC powder and are not expected to be present in materials where formation of SiC is the result of carbothermal reduction of silica in grain boundary glass. The magnitude of residual stresses and their influence on fracture toughness in such materials has yet to be determined, but can be expected to be lower than that in the composite with "clean" inclusion-matrix grain interfaces.

Room temperature flexure strength of the SNYC1 nanocomposite was significantly lower than that of the monolithic sample SNY (Table 2). In contrast, Weibull modulus is much higher—29.9 in comparison with 12.3 for monolithic silicon nitride. This can be easily understood if one takes into account the presence of carbon rich clusters with diameters around 15 μm, (Fig. 4) which act as fracture origins. Direct experimental evidence was given in the fractographic study of the SNYC1 material, where fracture of testing bars always originated at the carbon rich cluster.[16] The presence of clusters thus effectively reduces the strength. On the other hand, the cluster diameter distribution is very narrow, resulting in negligible variation of the flexural strength values. In order to increase the room temperature strength of such materials, further optimisation of the processing route will be necessary, which would allow complete elimination of free carbon from the material, or at least reduction in size of the free carbon clusters. The proposed way is to add carbon in the form of an organic precursor (e.g. sacharose, soluble phenolic resins etc.), which yields carbon as a result of pyrolytic cracking in the absence of oxygen. Under proper conditions, such a process could yield ultrafine amorphous carbon film homogeneously coating the silicon nitride matrix grains and readily reacting with silica. On the

Table 2
Room temperature mechanical properties of the micro/nanocomposites and reference samples

Sample	K_{IC}/MPa.m$^{1/2}$	σ/MPa	Weibull modulus
SNY	7.1	870	12.3
SNY20	6.4	710	–
SNYC1	5.5±0.2	390	29.9
SNYC2	6.1±0.2	n.m.	–

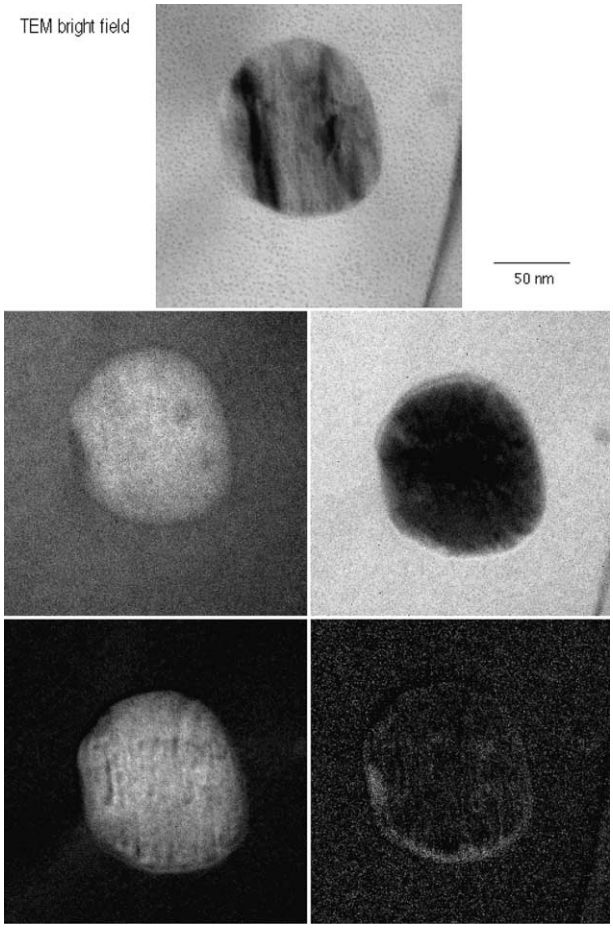

Fig. 3. The bright field TEM image of the SiC nanoinclusion within the Si_3N_4 grain and the EFTEM maps of Si, N, C, and O in, and around the inclusion.

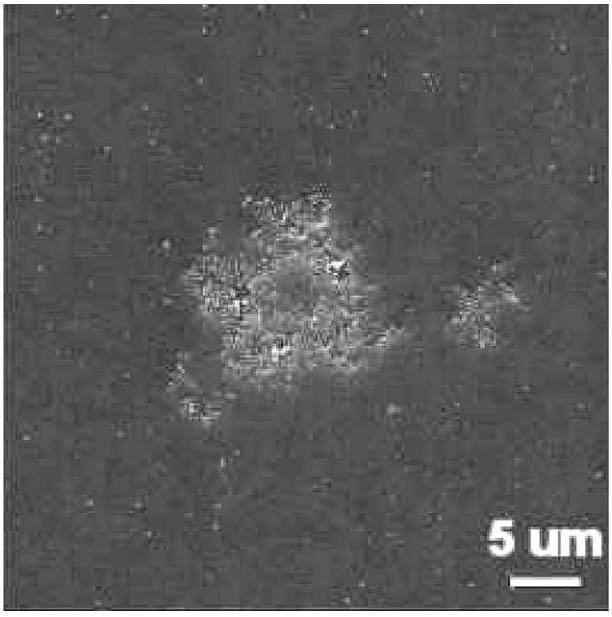

Fig. 4. Carbon-rich cluster in the Si_3N_4–SiC micro/nano composite.

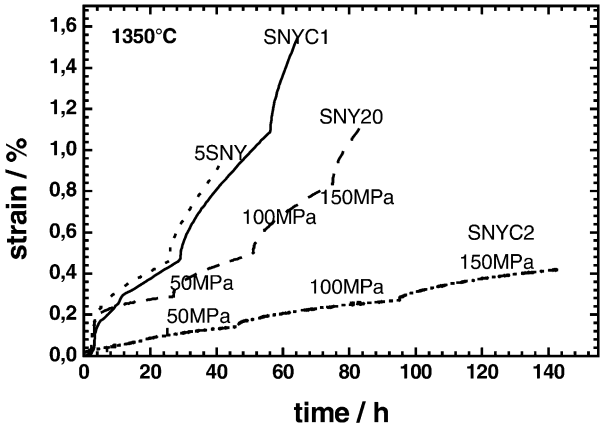

Fig. 5. Creep curves of tested specimens at 1350 °C.

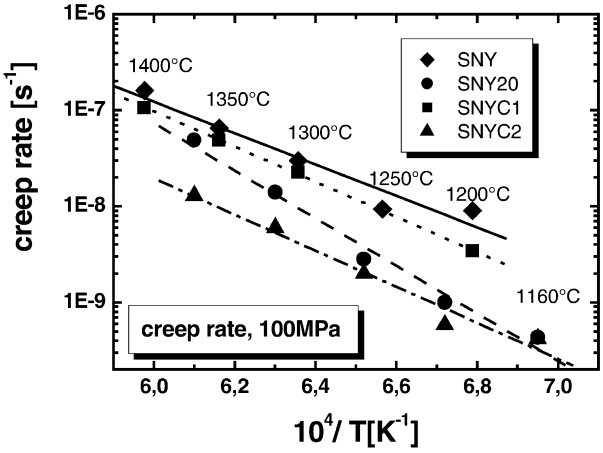

Fig. 6. Strain rates of the tested nanocomposite materials as a function of reciprocal temperature.

other hand, such a process would require further optimisation of the processing route due to the necessity of proper outgasing of various hydrocarbons, which form in the course of pyrolytic conversion of the organic precursor to carbon.

3.3. HT mechanical properties

The strain curves recorded during the creep tests of the micro/nano composites and the monolithic Si_3N_4 reference sample are shown in Fig. 5. Obviously, the lowest creep resistance has been detected for the monolithic sample, with slight improvement with the SNYC1. However, this was not significant, and the second reference, the specimen SNY20, performs much better, with only 0.5% strain after 24 h at 100 MPa load compared to more than 1% for both the SNY and SNYC1. The best results yield the SNYC2 material with only 0.4% strain after 150 h testing at 1350 °C with stepwise load increase from 50 to 150 MPa after each 50 h of testing. The creep rates at 100 MPa of all tested samples plotted as a function of reciprocal absolute temperature are shown in Fig. 6. At 1200 and 1350 °C the rates of deformation of the reference monolithic SNY sample are respectively 15 and 7 times higher than those of the SNYC2 nanocomposite. If compared with the reference nanocomposite SNY20, the creep rate at 1200 °C of the SNYC2 is approximately the same. However this specimen performs much better at 1350 °C, where the rate of deformation is three times lower than that of the SNY20. Our previous results suggest, that elimination of silica from the grain boundary phase by reaction with free carbon and accompanied by formation of nano-inclusions SiC changes the controlling mechanism of creep from grain boundary weakening to diffusion controlled creep.[4] This was most pronounced for the SNY20 composite and at lower temperatures, where the creep rates were most significantly reduced. The difference was not that obvious at higher temperatures, and at 1350 °C the creep rate of the monolithic SNY material was only 1.8 times higher than the rate of deformation of the composite. However, the material SNYC20 retains excellent resistance to high temperature deformation also in this temperature region, despite the fact the content of SiC nanoinclusions is far below the reported optimum value 10–15 wt.% of SiC.[3] It is suggested, that the creep resistance is increased by a combination of at least two factors. These include higher refractoriness of the grain boundary phase due to elimination of silica by reaction with carbon and the hindrance of grain boundary sliding by the pinning effect of intergranular particles, or by compressive stresses imposed by the presence of intragranular inclusions SiC. The detailed investigation of the mechanisms responsible for the retained high creep resistance is recently in progress.

4. Conclusions

Nearly fully dense micro/nano Si_3N_4/SiC composites have been prepared by *in situ* carbothermal reduction of silica within the ceramic body. Carbon, as silica-reducing and SiC-forming agent has been added in the form of soot. A specific heating schedule has been designed in order to prepare the composite and to complete the carbothermal reduction and the outgassing of reaction products (CO) before the densification of the composite was finished. Fracture toughness of the composites was slightly lower than that of the monolithic Si_3N_4 reference material and the flexural strength was significantly decreased due to the presence of carbon-rich clusters acting as fracture origins. Significant improvement of room-temperature mechanical properties can be achieved by further optimisation of the processing route, e.g. the heating schedule, or different source of carbon (organic precursor of C, for example). An excellent creep resistance has been achieved for the

composite sample containing approx. 5wt.% of SiC inclusions, which could be retained up to 1350 °C. The study of mechanisms controlling the creep is recently in progress.

Acknowledgements

Present work was partly supported by the National Slovak Grant Agency VEGA, project No. 2/5118/99, by the Slovak-German R&D Program, project X292.11. P, and by the NATO SfP Programe under the contract No. 97 41 22. The authors wish to express their thanks to P. Warbichler and F. Hofer from the Technical University Graz, Austria for the TEM measurements and to M. Kašiarová and J. Dusza from the Institute of Materials Research, Slovak Academy of Sciences, Košice, Slovakia, for determination of mechanical properties.

References

1. Niihara, K., New design concept of structural ceramics–ceramic nanocomposites. *J. Jpn. Ceram. Soc.*, 1991, **99**, 974–982.
2. Herrmann, M., Schubert, C., Rendtel, A. and Hübner, H., Silicon nitride/silicon carbide nanocomposite materials: I, fabrication and mechanical properties at room temperature. *J. Am. Ceram. Soc.*, 1998, **81**(5), 1094–1108.
3. Rendtel, A., Hübner, H., Herrmann, M. and Schubert, C., Silicon nitride/silicon carbide nanocomposite materials: II, hot strength, creep, and oxidation resistance. *J. Am. Ceram. Soc.*, 1998, **81**(5), 1109–1120.
4. Šajgalík, P., Hnatko, M., Lofaj, F., Hvizdoš, P., Dusza, J., Warbichler, P., Hofer, F., Riedel, R., Lecomte, E. and Hoffmann, M. J., SiC/Si_3N_4 nano/micro-composite–processing, RT and HT mechanical properties. *J. Eur. Ceram. Soc.*, 2000, **20**, 453–460.
5. Galusek, D., Reschke, S., Riedel, R., Dreßler, W., Šajgalík, P., Lenčéš, Z. and Majling, J., In situ carbon content adjustment in polysilazane derived amorphous SiCN bulk ceramics. *J. Eur. Ceram. Soc.*, 1999, **19**, 1911–1921.
6. Levin, E. M., Robbins, C. R. and McMurdie, H. F., Fig. 2388. In *Phase diagrams for ceramists*, ed. M. K. Reser. American Ceramic Society, Columbus, OH, 1969.
7. Hnatko, M., Šajgalík, P., Lenčéš, Z., Salamon, D. and Monteverde, F., Carbon reduction in the Y_2O_3–SiO_2 glass system at high temperature. *J. Eur. Ceram. Soc.*, 2001, **21**, 2797–2801.
8. Shetty, D. K., Wright, I. G., Mincer, P. M. and Clauer, A. H., Indentation fracture of WC–Co cermets. *J. Mater. Sci.*, 1985, **20**, 1873–1882.
9. Krstic, V. D., Production of fine, high-purity beta silicon-carbide powders. *J. Am. Ceram. Soc.*, 1992, **75**, 170–174.
10. JANAF. Thermochemical Tables 14. 1985, Suppl. 1.
11. Lièko, T. and Šajgalík, P., Preparation of α-Si_3N_4 powder and ceramics reinforced by β-Si_3N_4 whiskers. *Ceramics–Silikáty*, 1991, **35**, 127.
12. Šajgalík, P., Hnatko, M. and Lenčéš, Z., Properties of silicon nitride/carbide nano/micro composites—role of SiC nanoinclusions and grain boundary chemistry. In *Ceramic Materials and Components for Engines*, ed. J. G. Heinrich and F. Aldinger. Wiley-VCH Verlag GmbH, Weinheim, Germany, 2001, pp. 553–558.
13. Šajgalík, P., Hnatko, M. and Lenčéš, Z., Silicon nitride/carbide nano/micro composites for room as well as high temperature applications. *Key Eng. Mater.*, 2000, **175-176**, 289–300.
14. Nandy, M.-O., Schmauder, S., Kim, B.-N., Watanabe, M. and Kishi, T., Simulation of crack propagation in alumina particle-dispersed SiC composites. *J. Eur. Ceram. Soc.*, 1999, **19**, 329–334.
15. Sasaki, G., Suganuma, K., Fujita, T., Hiraga, K. and Niihara, K., Interface structure of Si_3N_4 matrix composite with nano-meter scale SiC particles. *Mar. Res. Symp. Proc.*, 1993, **287**, 335–340.
16. Kašiarová, M., Dusza, J., Hnatko, M., Lenčéš, Z. and Šajgalík, P., Mechanical properties of recently developed Si_3N_4–SiC nanocomposites. *Key Eng. Mater.*, 2002, **223**, 233–236.